RESEARCH ARTICLE

Microscopic Analysis of Flow Resistance of Oil Displacement Fluid in Reservoir Fractures

Wusheng Li[1] **and Junying Liao**[2,*]

[1] Directional Well Drilling Company of Bohai Drilling Engineering Co., Ltd, CNPC, Tianjin 300385, China
[2] Faculty of Engineering, China University of Petroleum-Beijing at Karamay, Karamay 834000, China

Abstract

The flow resistance of displacement fluids within reservoir fractures directly influences oil recovery efficiency and sweep efficiency, thereby exerting a substantial impact on reservoir recovery and overall oilfield production. To address the significant flow resistance of contemporary displacement fluids, this study developed a multi-performance evaluation apparatus capable of simultaneously measuring fluid viscosity, flow resistance, and displacement efficiency. The effects of various reservoir parameters and fluid compositions on flow resistance and sweep area were systematically analyzed. Elevated reservoir temperatures clearly reduce fluid flow resistance within fractures, allowing displacement fluids to penetrate more deeply into the reservoir. In contrast, an inverse relationship between reservoir pressure and flow resistance was observed, which poses a significant barrier to reducing flow resistance and achieving rapid fluid penetration. Moreover, through a micromolecular perspective and adsorption theory, this study identifies strategies to modify flow resistance, thereby substantially enhancing displacement efficiency and sweep area by lowering flow resistance. This study provides foundational data and a theoretical framework for mitigating fluid flow resistance within reservoir fractures during oil recovery, thereby facilitating enhanced oil recovery over a larger reservoir area.

Keywords: geological exploration, reservoir flooding, reservoir transformation, energy extraction, petroleum geology.

1 Introduction

The global economy is inextricably linked with the use of fossil fuels, which invariably imposes considerable constraints and creates synergistic development challenges for economic development and social progress [1]. The depletion of fossil energy resources and declining reservoir recovery rates have had a detrimental effect on global economic growth, and human civilisation is increasingly constrained by energy shortages [2]. The present situation is such that the supply of energy has become a major challenge, being actively addressed by many scientists. This has resulted in the development of diverse interdisciplinary fields, such as new energy science and engineering, energy and power engineering, and materials science and engineering [3, 4]. Moreover, the

Submitted: 19 November 2025
Accepted: 09 January 2026
Published: 15 January 2026

Vol. 2, **No.** 1, 2026.
10.62762/RS.2025.837826

***Corresponding author:**
✉ Junying Liao
2024216931@st.cupk.edu.cn

Citation
Li, W., & Liao, J. (2026). Microscopic Analysis of Flow Resistance of Oil Displacement Fluid in Reservoir Fractures. *Reservoir Science*, 2(1), 16–33.

identification and investigation of alternative energy sources has been shown to progressively reverse the economic stagnation caused by fossil energy shortages. The utilisation of clean energy sources, such as photovoltaics and wind power, is indisputably a potent catalyst for economic development and environmental protection [5]. While renewable energy sources have the potential to effectively supplement traditional fossil energy sources, numerous limitations exist that hinder their rapid replacement [6, 7]. Primarily, the low energy conversion efficiency of photovoltaics and wind power is inadequate in meeting the current surge in electricity demand, which is undoubtedly a key obstacle to the rapid and iterative development of renewable energy. Moreover, the inherently variable power generation efficiency of photovoltaics and wind power cannot ensure a consistent supply for standard production, which is inherently subject to factors such as sunlight and climate. Furthermore, the low storage efficiency of energy storage devices also prevents them from providing sufficient clean electricity at night or in windless conditions [8, 9]. This necessitates that scientists actively explore new materials with the objective of enhancing storage capacity. The high extraction efficiency of fossil fuels, including oil and natural gas, continues to be a pivotal factor in sustaining rapid global economic growth. A plethora of scientific researchers have proposed a multitude of novel solutions to address the current suboptimal extraction efficiency [10].

Reservoir stimulation, a pivotal measure currently employed to enhance the efficiency of fossil energy extraction from geological reservoirs, has unmistakably directly catalysed the accelerated growth of the global economy. Presently, flooding constitutes the most prevalent reservoir stimulation method, having been extensively utilised in the context of crude oil production across a multitude of oilfields, encompassing both conventional and unconventional low-permeability reservoirs [11, 12]. The efficacy of flooding for tertiary oil recovery has been demonstrated by the high actual production rates achieved. Moreover, the implementation of water injection, a technique employed in flooding operations, has been demonstrated to achieve high recovery efficiency while concurrently reducing costs. This approach has also been shown to maintain formation pressure stability by way of external water pressure, thereby extending the reservoir's development life [13, 14]. However, the addition of chemicals such as thickeners and crosslinkers during flooding has been demonstrated to result in reservoir damage. It has been demonstrated that reservoir phenomena, including but not limited to fingering and channeling, which are a consequence of heterogeneous reservoirs, have the capacity to reduce sweep efficiency. It has been demonstrated that substantial quantities of crosslinked flooding fluid can readily form gel masses that effectively seal fractures, thereby causing damage to the geological reservoir. This has the effect of hindering fracture connectivity and the flow of crude oil. Furthermore, chemicals adsorbed on rock have also been shown to dissolve in groundwater, with the potential to contaminate the reservoir water [15, 16]. Furthermore, the adsorption of chemicals onto reservoir rocks has been shown to result in the clogging of fractures and the contamination of groundwater. In addition, the flow resistance of the displacement fluid within the reservoir fractures is increased due to the strong adsorption properties of the chemicals. The reduction of flow resistance caused by chemical adsorption, in addition to the development of devices and methods to assess this flow resistance, are currently major challenges that must be addressed [17, 18]. It is anticipated that this will provide fundamental data and theoretical support for the efficient extraction of reservoir energy. The present research is chiefly concerned with the flow mechanism, the influencing factors, and the optimisation techniques of fractured reservoirs. Furthermore, scientific research is underway to explore the potential of a novel oil displacement fluid (CO_2) that has the capacity to substitute for water. Despite the fact that the low flow resistance of CO_2 fluid can circumvent substantial impediments engendered by water flooding, its inadequate proppant carrying capacity and elevated frictional resistance nevertheless serve to circumscribe the extent of its application [19, 20]. Petroleum engineers are utilising machine learning and numerical simulation to explore the fluid resistance of geological reservoirs. However, the inherent limitations of this approach, namely the strong dependence on input data and the weak adaptability, have yet to be fully addressed, as they continue to impede the effective management of high friction in reservoir fluids [21, 22].

The present study constructed a multi-property coupled evaluation device for oilfield fluids over a wide viscosity range (0 mPa·s-250 mPa·s). This apparatus facilitates the real-time measurement of multiple properties, including fluid viscosity, phase state, fracture flow resistance, fracture propagation,

and reservoir damage. An equation for flow resistance was formulated in order to ascertain the differences in flow resistance of oil displacement fluids under varying conditions. This approach facilitates the identification of the most significant factors affecting flow resistance, thereby enabling subsequent process optimisation. Furthermore, microscopic intermolecular interaction models and adsorption theory were used to reveal the flow mechanisms that trigger flow resistance within reservoir fractures, providing fundamental mitigation strategies for improving flow resistance.

2 Materials and Methods

2.1 Preparation of Acrylamide Polymers

A mixture of 15 g of acrylic acid and 19.2 g of sodium 2-acrylamido-2-methylpropanesulfonate was prepared and poured into a three-necked flask containing 50 ml of distilled water. The mixture was then adjusted to a pH of 7 using sodium carbonate, ensuring precise control over the acidity level. Concurrently, the mixture was stirred at a speed of 200r/s, at which point 4.8g of monomer acrylamide, 2.7g of dimethyldiallylammonium chloride, 0.3g of OP-10 and 1.85g of didecylmethylallylammonium chloride were added, and the temperature was raised to 65°C. The mixture was then left to react for 7.5 hours. Following a cooling period to ambient temperature, the copolymer was subjected to an ethanol wash, then dried and crushed into 100-mesh solid particles. This process yielded a heat-resistant and salt-resistant double-tail hydrophobic oil displacement agent.

2.2 Flow Resistance in Reservoir Fractures

The flow resistance in reservoir fractures must account for the rheological parameters of the working fluid, including flow rate and viscosity, during polymer flooding. These parameters are essential for the calculation and analysis of flow resistance. Equation 1 (Forchheimer equation) presents the mathematical expression for determining the flow resistance of the flooding fluid within reservoir fractures. The relevant parameters can be defined and measured using the multi-functional coupling device illustrated in Figure 1. It is important to note that the fluid flow resistance in reservoir fractures is evaluated using pressure drop (Δp) as an indicator. A larger flow resistance therefore corresponds to a larger pressure drop value [23, 24].

$$\Delta p = \frac{\mu L}{k} u + \beta \rho L u^2 \tag{1}$$

where Δp is the fluid pressure drop in reservoir fractures, Pa. μ is the fluid viscosity of oil displacement fluid in reservoir fractures, mPa·s. L is the actual length of reservoir fractures, m. k is the permeability of reservoir rock, mD. u is the Darcy speed, m/s. β is the Non-Darcy coefficient, and it depends on the pore structure. ρ is the fluid density, kg/m^3.

The fluid viscosity, as depicted in Equation 1, can be measured and subsequently solved (Equation 2) by employing the capillary viscometer, as illustrated in Figure 1. In addition to measuring fluid viscosity, the capillary viscometer depicted in Figure 1 can also be utilised to evaluate and analyse the rheological index (Equation 3) and consistency coefficient. Furthermore, the multi-performance coupling device (see Figure 1) has been demonstrated to measure related performance parameters such as the phase state, displacement efficiency, core damage, and flow resistance of the oil displacement fluid. In addition to this, it is also capable of evaluating fluid rheological parameters [25, 26].

$$\mu = \frac{D \Delta p_{\text{pipeline}}}{8u/D} \cdot \frac{4L}{D} \tag{2}$$

$$\lg \tau_w = \lg K \left(\frac{3n+1}{4n} \right)^n + n \lg \left(\frac{8u}{D} \right) \tag{3}$$

where $\Delta p_{\text{pipeline}}$ is the pressure difference across the capillary, Pa. D is the inner diameter of the capillary, m. K and n are the viscosity coefficient and rheological index of oil displacement fluid. τ_w is the shear rate of oil displacement fluid, s^{-1}.

2.3 Fluid Mechanics Model of Fluid in Fractures

The fluid mechanics model in fractures during water flooding in geological reservoirs is principally constructed based on the law of conservation of mass, the law of conservation of momentum and Darcy's law. However, it is imperative that the actual geological reservoir conditions are also taken into consideration.

During water flooding in geological reservoirs, the fluid flow behavior within fractures is typically described using a dual-porosity model, which serves as the foundation for constructing the governing mechanical equations of fluid motion in the fracture network. This formulation involves the fluid dynamics equations for both the fracture (Equations 4) and the

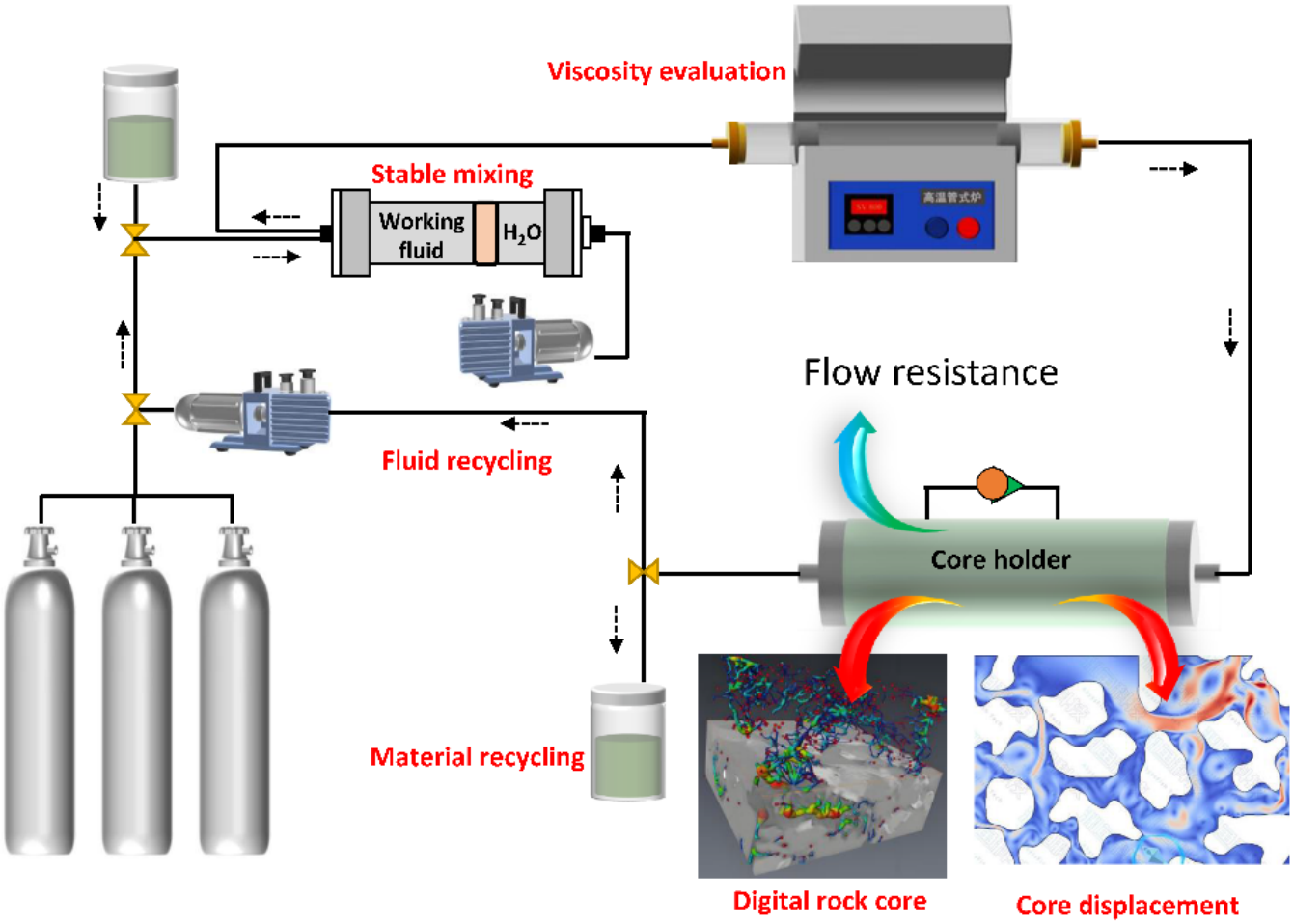

Figure 1. Multi coupling evaluation device for reservoir working fluid parameters.

matrix systems (Equations 5) [27, 28].

$$\frac{\partial(\phi_f \rho_f)}{\partial t} + \nabla(\rho_f u_f) = q_{mf} \tag{4}$$

$$\frac{\partial(\phi_m \rho_m)}{\partial t} + \nabla(\rho_m u_m) = -q_{mf} \tag{5}$$

where ϕ_f and ϕ_m represent the permeabilities of the fracture system and matrix system, respectively. ρ_f and ρ_m represent the densities of the fracture system and matrix system, respectively. u_f and u_m represent the seepage velocities of the fracture system and matrix system, respectively. q_{mf} is the exchange term of the matrix-fracture, and it can be usually calculated using the Kazemi formula shown in Equation 6 [29].

$$q_{mf} = \alpha \frac{k}{\mu}(\rho_m - \rho_f) \tag{6}$$

where α is the shape factor. μ is the viscosity of underground fluids.

In addition, to ensure numerical stability and continuity during the simulation of acidizing and fracture connectivity, the weak form of the reservoir fluid dynamics model was solved based on the dual-porosity framework (Equations 7 and Equations 8) [30].

$$\int_\Omega \omega_f \phi_f c_f \frac{\partial p_f}{\partial t} dV + \int_\Omega \nabla \omega_f \left(\frac{k}{\mu} \nabla p_f\right) dV = \int_\Omega \omega_f \frac{q_{mf}}{\rho} dV \tag{7}$$

$$\int_\Omega \omega_m \phi_m c_m \frac{\partial p_m}{\partial t} dV + \int_\Omega \nabla \omega_m \left(\frac{k}{\mu} \nabla p_m\right) dV = \int_\Omega \omega_m \frac{q_{mf}}{\rho} dV \tag{8}$$

where ω_m and ω_f are the testing functions for cracks and matrix. c_f and c_m are the compressive coefficient of cracks and matrix. V usually represents a volume element, which is a three-dimensional small volume in the computational domain Ω.

2.4 Multi Performance Evaluation Device for Reservoir Fluids

This multi-coupling experimental apparatus (Figure 1) is designed to simulate and evaluate the flow characteristics of reservoir geological fluids within fractured core systems, with a particular focus on assessing fluid viscosity, flow resistance, and displacement efficiency. The core component of the system is a high-pressure core holder capable of accommodating both natural and artificial fractured core samples. Target geological fluids—such as crude oil, water, or polymer solutions—are injected into the core through a precision high-pressure pump.

A temperature–pressure control module is integrated into the system to replicate in-situ reservoir conditions. Fluid viscosity is monitored in real time using an inline viscometer, while flow resistance is measured by a differential pressure transducer that records pressure gradient variations along the fracture channel. Displacement efficiency is evaluated through the outlet fluid collection system combined with mass balance calculations, supplemented by X-ray or CT imaging modules for visualizing fluid distribution within the core.

The multi-coupling mechanism enables synchronized parameter control and data integration via a real-time acquisition and analysis system, thereby facilitating a quantitative assessment of the influence of viscosity variations on flow resistance and displacement efficiency under simulated reservoir conditions.

2.5 Experimental Analysis of Displacement Efficiency

To evaluate the displacement efficiency during the water flooding process, a series of unidirectional core flooding experiments (Figure 1) were conducted under constant flow conditions using a laboratory core flooding apparatus. Natural sandstone cores were dried, vacuum-saturated, and characterized to determine porosity and permeability prior to the tests. After establishing the initial water saturation, the cores were saturated with simulated crude oil until a stable initial oil saturation was achieved. Subsequently, deionized water (or brine with a specified salinity) was injected into the cores at a constant flow rate, while the injected volume, produced oil and water volumes, and differential pressure were continuously recorded. The experiments were performed under constant temperature conditions and continued until the oil production rate became negligible. The cumulative oil recovery at various injected pore volumes (PV) was used to calculate the displacement efficiency, and recovery curves were plotted to analyze the effects of injection water properties and flow rate on the overall oil displacement performance.

2.6 Molecular Dynamics Model Construction of Adsorption Model

The adsorption model of oil displacement agents on mineral surfaces was constructed by cleaving representative surfaces, such as quartz and kaolinite, along the (001) crystallographic plane, followed by structural optimization. Surfactant or polymer molecules, together with water and ions (Na^+, Cl^- at 0.1 M), were positioned above the surface to replicate reservoir conditions. The COMPASS force field was applied to all components, and periodic boundary conditions were imposed in all directions. Energy minimization was initially performed using the steepest-descent algorithm, followed by equilibration under the NVT ensemble at 298 K for 200 ps, and subsequently under the NPT ensemble at 298 K and 1 atm for 500 ps to stabilize temperature and pressure. Production molecular dynamics simulations were then carried out for 2 ns with a time step of 1 fs in a simulation box of approximately $5 \times 5 \times 8\,\mathrm{nm}^3$. Adsorption behavior was analyzed through adsorption energies, density profiles, and radial distribution functions, providing insights into molecular orientation, adsorption layer thickness ($\sim$0.8 nm), and interfacial interaction strength ($\sim$25 kcal/mol per molecule).

The adsorption model based on molecular dynamics theory can calculate the adsorption energy (Eq. 9) to evaluate and reveal the flow resistance and transition mechanism in reservoir fractures under different factors.

$$E_{\mathrm{ads}} = E_{\mathrm{sys}} - (E_{\mathrm{sur}} + E_{\mathrm{adsorbate}}) \tag{9}$$

where E_{ads} is the adsorption energy. E_{sys} is the total energy of the oil displacement working fluid system. E_{sur} is the surface energy of reservoir rocks. $E_{\mathrm{adsorbate}}$ is the internal energy of isolated adsorbed molecules.

3 Results and Discussion

3.1 Fluid Viscosity During Oil Displacement in Reservoir Fractures

Previous studies have demonstrated an intrinsic relationship between fluid viscosity and flow resistance in geological reservoirs, as expressed in

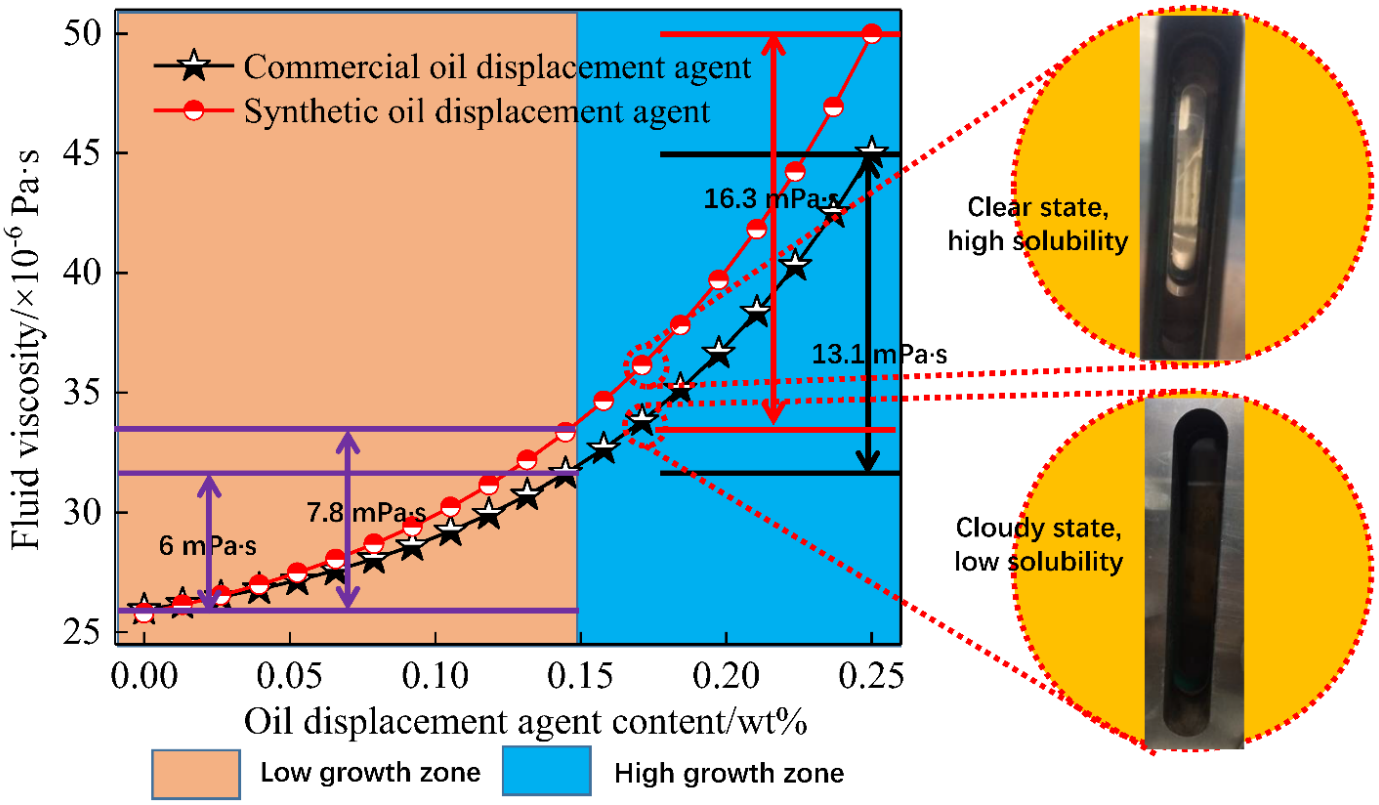

Figure 2. Changes in fluid viscosity of oil displacement fluid under different oil displacement agents.

Equation (1). The viscosity of oilfield working fluids employed for reservoir stimulation is influenced not only by reservoir parameters, such as pressure, temperature, and rock properties, but also by operational factors, including chemical additives, shear stress, and injection rate. These variations inevitably result in corresponding adjustments to the flow resistance of the working fluid within reservoir fractures.

3.1.1 Influence of working fluid composition on fluid viscosity

The introduction of a displacing agent into a geological reservoir can significantly enhance oil recovery efficiency. The concentration of the displacing agent plays a critical role in determining both fluid viscosity and the effectiveness of reservoir reconstruction. Figure 2 illustrates the influence of displacing agent concentration on fluid viscosity, including the corresponding viscosity variations observed for commercially available displacing agents under identical evaluation conditions.

Figure 2 illustrates that with increasing oil displacement agent concentration, the viscosity of fluids corresponding to both displacement agent types exhibits a nonlinear growth pattern, initially increasing gradually and subsequently accelerating. The synthetic oil displacement agent (red circles) induces a more pronounced rise in fluid viscosity, particularly at higher agent concentrations, whereas the commercial oil displacement agent (black stars) demonstrates a more gradual increase but enters the growth phase at lower concentrations. The figure further delineates a "low-growth zone" (light brown) and a "high-growth zone" (blue), representing a distinct transition in viscosity behavior: the low-growth zone shows minimal changes in viscosity, while the high-growth zone is characterized by a sharp increase. These observations underscore the influence of both displacement agent type and concentration on fluid viscosity, suggesting that although both synthetic and commercial agents are applicable in oil production and related processes, synthetic agents exhibit superior viscosity enhancement in terms of both growth rate and magnitude.

The curves depicting the variation of fluid viscosity with oil displacement agent concentration in Figure 2 can be divided into low-growth and high-growth regions. In the low-growth region, spanning 0.00 wt% to 0.15 wt%, the viscosity increases gradually. The curves are approximately linear or exhibit slight upward curvature, indicating that the initial addition of the displacement agent has a limited effect on

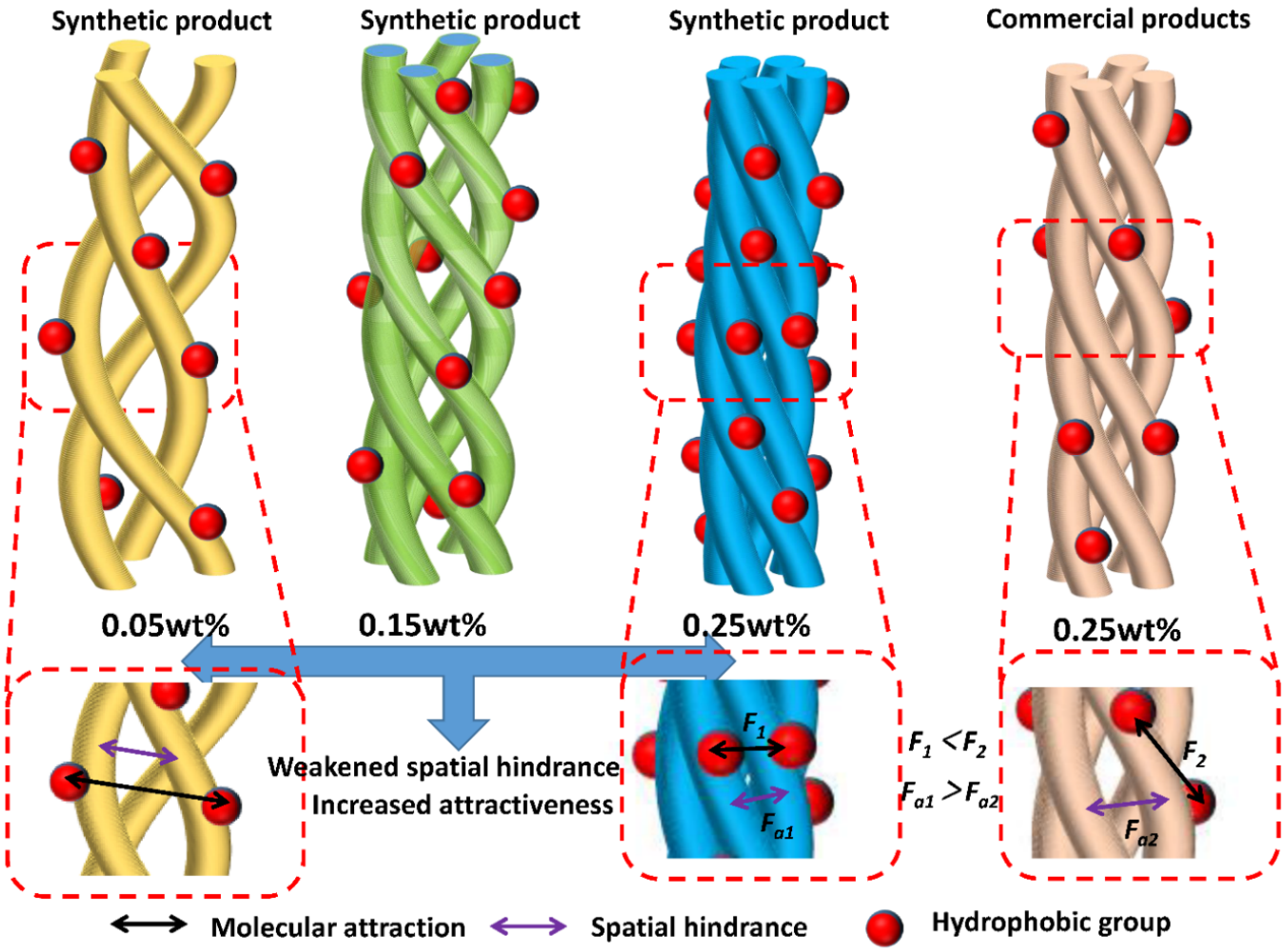

Figure 3. Molecular interactions between different types and contents of oil displacement agents.

fluid viscosity. Although both displacement agents display similar low-growth trends, subtle differences exist in the magnitude of viscosity increase. For the commercial oil displacement agent, the fluid viscosity rises modestly from 0.00 wt% to 0.05 wt%, reaching approximately 6 mPa·s. In contrast, at the same concentration, the synthetic displacement agent induces a higher viscosity increase, reaching 7.8 mPa·s. This relatively smaller increase in the commercial agent indicates that, while both agents enhance fluid viscosity, the initial changes in viscosity do not substantially impact the overall performance of the displacement fluid.

In the concentration range of approximately 0.15 wt% to 0.25 wt%, a pronounced increase in fluid viscosity is observed, which clearly contributes to enhanced reservoir reconstruction and production efficiency. The commercial displacing agent shows a steeper viscosity rise beginning at 0.15 wt%, with the viscosity increasing sharply to approximately 37 mPa·s at 0.20 wt%. When the concentration reaches 0.25 wt%, the viscosity further rises to about 45 mPa·s, corresponding to an overall increase of 13.1 mPa·s—more than twice the 6 mPa·s increment observed below 0.15 wt%. In contrast, the synthetic displacing agent exhibits an even more pronounced viscosity enhancement beyond 0.15 wt%. Between 0.15 wt% and 0.20 wt%, the fluid viscosity increases by approximately 40.6 mPa·s, indicating a much stronger thickening capability. As the concentration continues to rise to 0.25 wt%, the viscosity rapidly increases to 50.2 mPa·s. This remarkable viscosity growth highlights the superior rheological modification performance of the synthetic displacing agent compared with the commercial counterpart, particularly in the high-concentration regime.

The positive correlation between displacing agent concentration and fluid viscosity primarily arises from the increased charge density on displacing agent molecules (Figure 3), which enhances electrostatic repulsion between molecular chains and promotes the stretching of macromolecular structures within

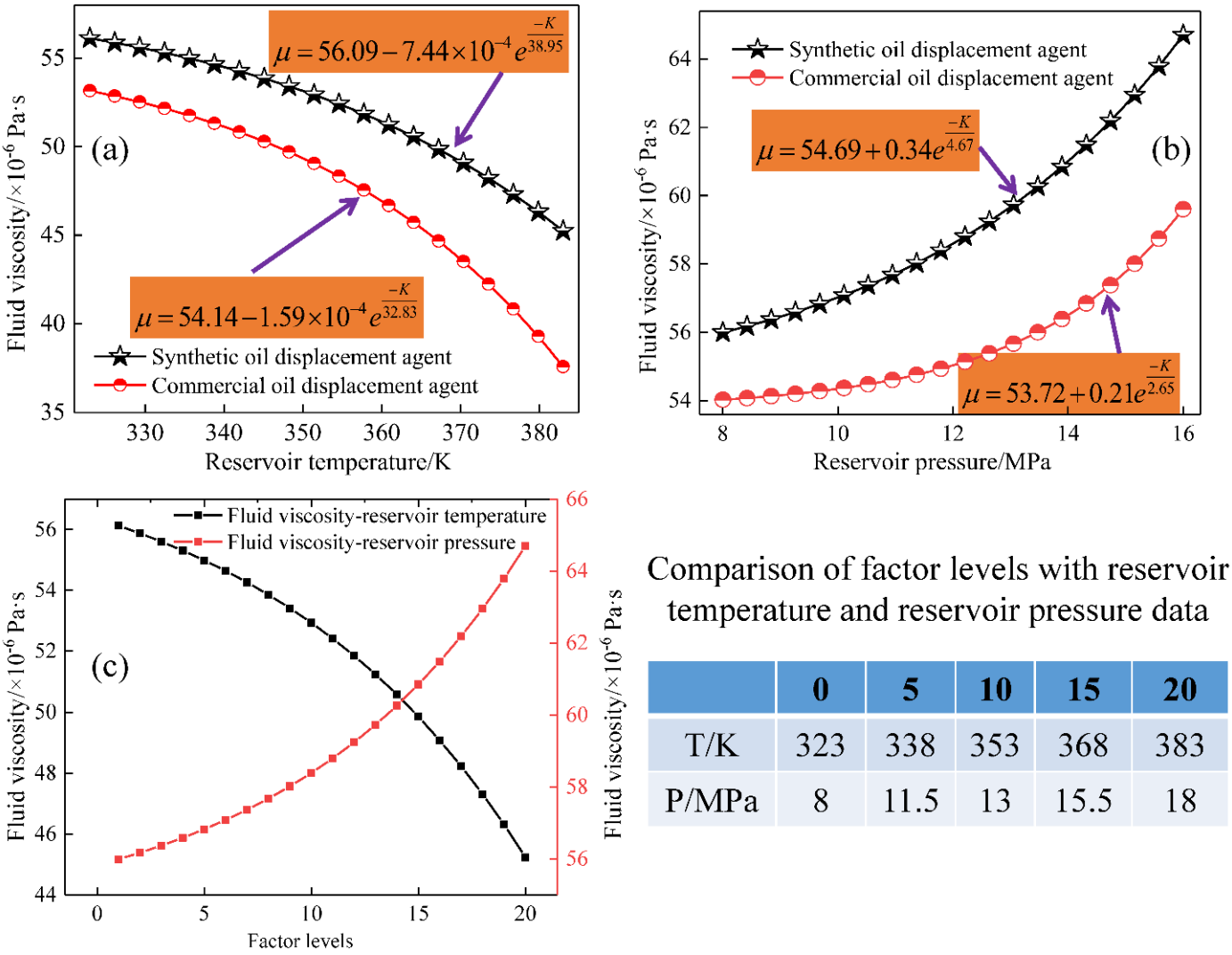

Comparison of factor levels with reservoir temperature and reservoir pressure data

	0	5	10	15	20
T/K	323	338	353	368	383
P/MPa	8	11.5	13	15.5	18

Figure 4. Effects of reservoir temperature and pressure on the viscosity of oil displacement fluids containing oil displacement agents. (a) Reservoir temperature. (b) Reservoir pressure. (c) Synthetic oil displacement agent.

the displacement fluid. Moderate intermolecular stretching facilitates higher fluid viscosity, as greater molecular repulsion and chain extension occur with increasing displacing agent concentration. Moreover, the more pronounced viscosity enhancement observed for the synthetic displacing agent at equivalent concentrations is mainly attributed to its double-tailed molecular architecture [31, 32]. This structural configuration reduces steric hindrance and improves molecular solubility, thereby allowing more effective intermolecular interactions and network formation. In contrast, the linear long-chain structure of commercial displacing agent introduces significant steric hindrance and limited solubility, which suppresses molecular mobility and weakens intermolecular association. Consequently, the commercial displacing agent exhibits a comparatively smaller increase in fluid viscosity [33, 34].

3.1.2 Influence of reservoir temperature and reservoir pressure on fluid viscosity

Temperature and pressure, as the fundamental geological parameters within a reservoir, exert a pronounced influence on the viscosity of the working fluid within fractures, thereby directly affecting the reservoir reconstruction capacity and the oil recovery efficiency of the displacement system. Figure 4 presents the variations in the viscosity of the displacement fluid under different reservoir temperatures and pressures, providing a theoretical basis for selecting an optimal displacement fluid corresponding to the target reservoir conditions.

Reservoir temperature and displacement fluid viscosity exhibit an inverse relationship, whereas fluid viscosity increases with increasing reservoir pressure. Although the effects of temperature and pressure on viscosity display distinct trends, both parameters

induce relatively minor variations at lower values (i.e., low temperature and low pressure). Figure 4 clearly demonstrates that reservoir temperatures below 353 K lead to minimal changes in the rheological viscosity of the displacement fluid, with only a 3.2 mPa·s reduction observed when the temperature increases from 323 K to 353 K. This limited viscosity decline reflects the strong temperature resistance of the displacement fluid under low-temperature conditions, which is particularly advantageous for near-wellbore and shallow reservoir recovery applications. However, when the temperature exceeds 353 K, the viscosity decreases more sharply, with a 7.4 mPa·s reduction as the temperature rises from 353 K to 383 K. This observation indicates the relatively weak rheological stability of the displacement fluid under high-temperature reservoir conditions.

In comparison with the synthetic oil-displacing agent, the commercial oil-displacing agent demonstrates a more significant reduction in viscosity under equivalent reservoir temperature conditions. When the reservoir temperature is below 353 K, the rheological viscosity of the displacement fluid decreases from 53 mPa·s to 49 mPa·s. It is evident that, the viscosity reduction exhibited by the fluid containing the commercial oil-displacing agent (4.0 mPa·s) is considerably more pronounced in comparison to that observed for the synthetic counterpart under comparable temperature conditions,. However, when the reservoir temperature exceeds 353 K, the fluid viscosity decreases more sharply, with a drop of approximately 11.2 mPa·s. This indicates the inferior thermal resistance and rheological stability of the commercially available oil-displacing agent at elevated temperatures.

Figure 4 further illustrates the positive correlation between the apparent viscosity of both fluids and reservoir pressure, offering valuable insights for evaluating the oil recovery efficiency of deep, low-permeability reservoirs. Despite the contrary variations in pressure and temperature within the reservoir, both viscosity-pressure curves can be delineated into two distinct regions. At lower pressures ($P < 12$ MPa), the increase in fluid viscosity is relatively limited (approximately 2.6 mPa·s), suggesting that moderate-pressure reservoirs provide stable rheological behaviour under constant temperature conditions. Conversely, when the reservoir pressure exceeds 12 MPa, a marked exponential increase in viscosity (approximately 6.1 mPa·s) is evident, suggesting that elevated pressure enhances the rheological performance and overall stability of the displacement fluid. However, the fluid containing the commercially available oil-displacing agent exhibits a relatively weak response to pressure variation, with only a modest viscosity increase of about 5.4 mPa·s as pressure rises from 8 MPa to 16 MPa. This limited sensitivity may be attributed to the different intermolecular interactions and molecular configurations of the two oil-displacing agents under varying pressure conditions.

The effects of reservoir temperature and pressure on the apparent viscosity of displacement fluids containing oil-displacing agents are primarily governed by variations in intermolecular interactions, which can be attributed to the proximity of hydrophobic groups and the steric hindrance of molecular chains [35]. As the reservoir temperature increases, molecular motion intensifies, inevitably enhancing the steric hindrance among displacement agent chains. Concurrently, elevated temperature also increases the intermolecular spacing between hydrophobic groups within the displacement agent molecules. The weakened hydrophobic interactions, together with the enhanced molecular mobility, reduce the density of intermolecular cross-linking within the microscopic network [36]. Consequently, both increased steric hindrance and enlarged intermolecular spacing contribute to a decrease in the microscopic grid density of the displacement fluid, leading to a reduction in its macroscopic viscosity. In particular, the single linear-chain structure of commercially available crosslinkers tends to induce greater steric hindrance under high-temperature conditions, thereby further diminishing the microscopic grid density and exacerbating the viscosity loss of the displacement fluid.

Reservoir pressure compresses the intermolecular spacing within the displacement fluid, forcing molecules that were initially separated by larger distances to move closer together under external stress, thereby forming a denser three-dimensional network structure [37, 38]. Simultaneously, the applied pressure promotes the formation of new intermolecular interactions—particularly between hydrophobic groups—that were previously too distant to bond under ambient conditions. This enhanced molecular packing and the emergence of additional interactions increase both the microscopic network density and the macroscopic viscosity of the displacement fluid. In contrast, commercially available oil-displacing agents, which possess relatively smaller

hydrophobic groups, exhibit limited capacity to generate new intermolecular associations under elevated pressure. Consequently, their viscosity enhancement and sensitivity to reservoir pressure are significantly lower than those of synthetic oil-displacing agents.

It is evident that variations in the viscosity of displacement fluids are governed not only by their formulation but also by reservoir conditions, particularly temperature and pressure. These conditions have been shown to be critical determinants of fluid rheology. Consequently, the selection of appropriate reservoir conditions for different geological formations can be guided by the corresponding data presented in Figures 3 and 5. Furthermore, the comprehensive evaluation of viscosity-influencing factors provides a mechanistic foundation for understanding and predicting the flow resistance behaviour of residual or undisplaced fluids within reservoir fractures.

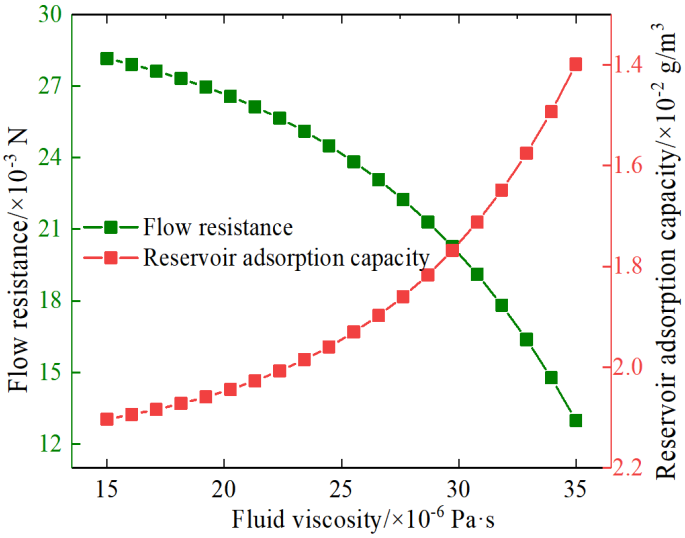

Figure 5. Relationship curve between oil displacement fluid viscosity, flow resistance and reservoir adsorption capacity.

3.2 Flow Resistance of Reservoir Fluid in Fractures

3.2.1 Influence of fluid viscosity on the flow resistance

The displacement efficiency of working fluids in geological reservoirs is subject to a gradual decline due to reservoir resistance, thereby exerting a substantial impact on EOR. Furthermore, the flow resistance of working fluids in reservoir fractures is influenced by both the working fluid and reservoir factors. Therefore, the initial exploration was conducted to investigate fluid viscosity. The effects of reservoir fluids and reservoir factors on flow resistance are demonstrated in Figure 5. This is a crucial factor in the selection of suitable displacement fluids for geological reservoirs.

Figure 5 illustrates a distinct inverse relationship between fluid viscosity and flow resistance, whereby lower-viscosity fluids exhibit markedly higher flow resistance. In contrast, an increase in viscosity results in a significant reduction in flow resistance, which consequently impedes the enhancement of reservoir recovery efficiency. This inverse correlation is not only governed by the microscopic mesh density of the displacement fluid but also closely linked to the adsorption behavior of fluid molecules on the rock surface, ultimately leading to variations in flow resistance. Previous studies have demonstrated that high-viscosity reservoir fluids tend to form denser microscopic network structures (Figure 3), whereas lower mesh densities correspond to weaker fluid viscosities. These microscopic networks originate from intermolecular interactions and chemical bonds formed between functional groups (particularly hydrophobic groups) on the displacement agent molecules [39]. At lower viscosities, the reduced number of intermolecular bonds results in a greater proportion of free functional groups. These unbonded groups readily interact with hydrophobic sites on the rock surface, generating additional drag forces and entraining a larger portion of the displacement fluid. Consequently, the increased drag induced by the abundance of free functional groups leads to higher overall flow resistance, as shown in Figure 6. However, the increase in oil displacement fluid viscosity occurs at the expense of a large number of functional groups that participate in forming extensive chemical bonds and microscopic network structures [40]. The resulting reduction in free functional groups weakens the interfacial interactions between fluid molecules and the rock surface. This diminished interaction in high-viscosity fluids not only reduces the extent of molecular adsorption on reservoir rock surfaces but also effectively mitigates flow resistance by decreasing molecular drag forces.

Therefore, while fluid viscosity is the apparent cause of the reduced flow resistance of the displacement fluid, the fundamental cause of the change in flow resistance is the adsorption of the displacement agent molecules on the rock surface and the drag of the microscopic grid. As demonstrated in Figure 5 and Table 1, a clear causal relationship is evident between fluid viscosity, adsorption capacity, and drag force.

Table 1. Data analysis of the relationship between fluid viscosity and adsorption energy.

Fluid viscosity/ mPa·s	10	20	30	40	50
drag force, × 10^{-3} N	5.3	5.1	4.7	4.0	3.2
Adsorption energy, × 10^{-4}J/mol	3.8	3.7	3.5	3.1	2.4

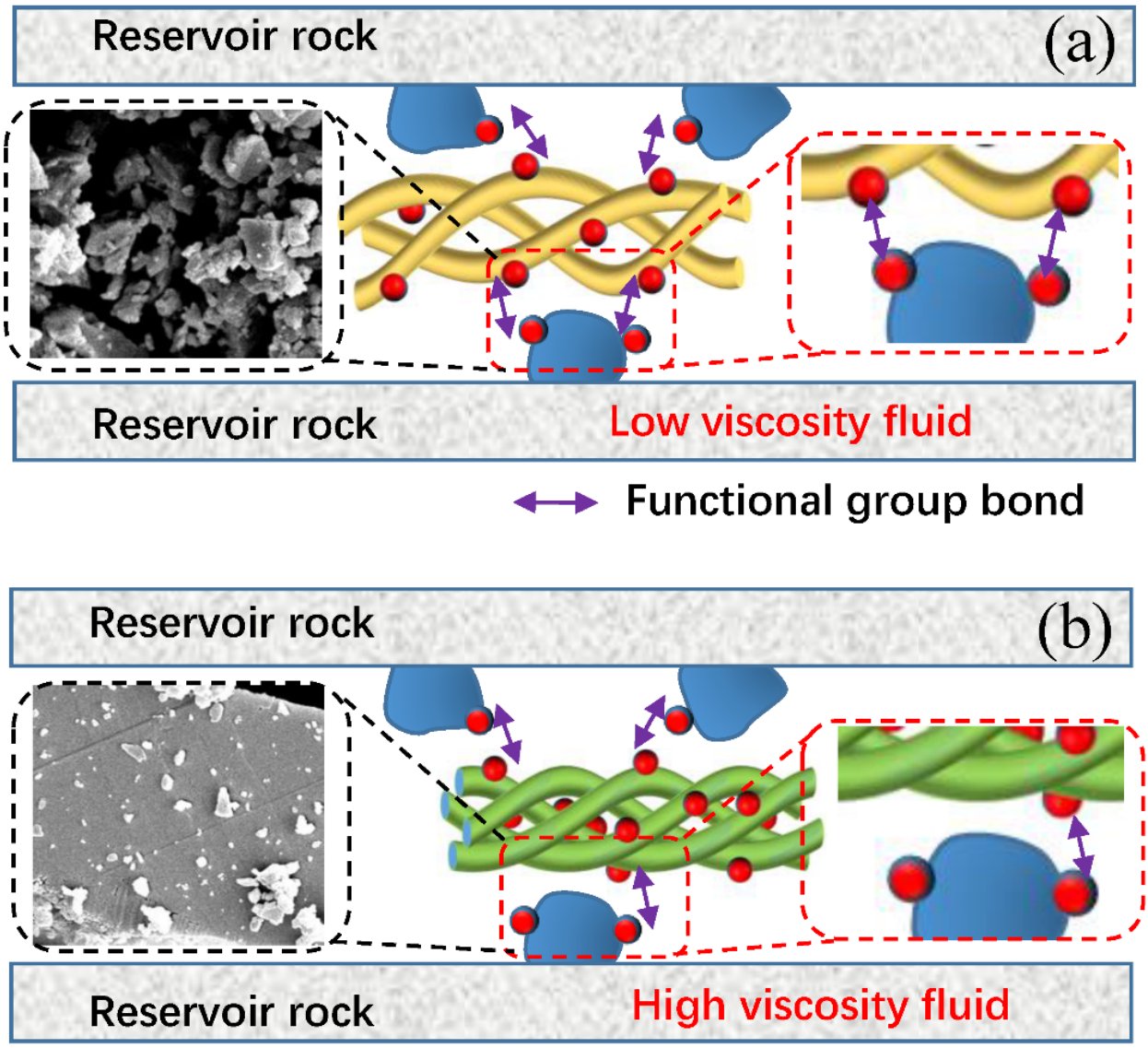

Figure 6. Microscopic effects of oil displacement fluids with different fluid viscosities in reservoir fractures.

3.2.2 Influence of rock roughness on the flow resistance

The surface roughness (JRC) of reservoir fractures exerts a pronounced influence on the flow resistance of displacement fluids within the fracture network, as illustrated in Figure 7. As shown, smooth fracture surfaces exhibit negligible flow resistance, whereas increased surface roughness significantly impedes the movement of displacement fluids within reservoir fractures. When the fracture surface roughness is 2, the flow resistance of the displacement fluid is approximately 28 × 10^{-3} N; increasing the roughness to 5 results in only a minor increase of 2 × 10^{-3} N. This slight rise indicates that fractures with low to moderate roughness have minimal influence on fluid flow, and their impact on enhanced oil recovery (EOR) is therefore negligible. However, when the surface roughness reaches 8, the flow resistance increases sharply to 35 × 10^{-3} N. This pronounced escalation can be attributed to multiple factors. At low roughness, the displacement fluid typically exhibits laminar or weakly turbulent flow behavior at low flow velocities, leading to limited variation in flow resistance. In contrast, higher roughness intensifies fluid perturbations, inducing vortex formation and

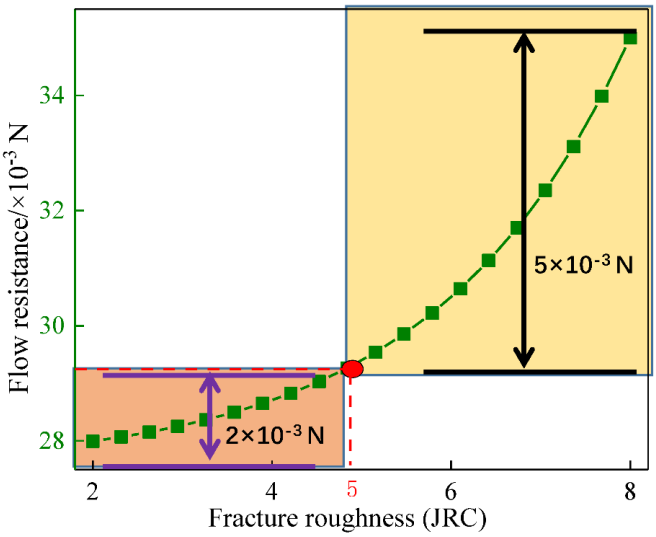

Figure 7. Effect of rock roughness of different fracture surfaces on flow resistance of oil displacement fluid.

local stagnation zones that facilitate the accumulation of residual foam. The coexistence of turbulence and foam substantially disrupts the continuity of flow within reservoir fractures, thereby markedly increasing the flow resistance of the displacement fluid. Furthermore, the increased roughness of the rock surface directly enhances the number of available adsorption sites for chemical molecules, thereby intensifying molecular drag and the overall flow resistance of the displacement fluid within the reservoir [41, 42]. In addition, greater surface roughness expands the boundary layer thickness along the rock interface, leading to an increased velocity gradient within the near-wall region [43, 44]. A larger velocity gradient under identical flow conditions results in a reduced effective flow rate of the displacement fluid, which serves as a macroscopic manifestation of elevated flow resistance in rough-walled reservoir fractures (Figure 8).

3.2.3 *Influence of rock porosity and pore radius on the flow resistance*

The rheological properties of displacement fluids are also affected by the geological parameters of reservoir rocks. As shown in Figure 9, flow resistance exhibits an inverse relationship with rock porosity, offering guidance for selecting suitable displacement fluids under varying geological conditions. Although resistance generally decreases with increasing porosity, the rate of decline differs across porosity ranges. When rock porosity is below 8%, flow resistance changes only slightly—from 33×10^{-3} N at 4% to 31×10^{-3} N at 8%. However, when porosity exceeds 8%, resistance decreases rapidly, reaching 26×10^{-3} N at 12%.

The positive correlation between porosity and fluid resistance in reservoir fractures arises mainly from adsorption and fracture connectivity. At low porosity, the larger contact area between the displacing fluid and the fracture surface enhances adsorption capacity, thereby increasing viscous drag and flow resistance under the same injection pressure [45, 46]. Moreover, low porosity reduces fracture connectivity, restricting fluid migration to limited flow channels and hindering penetration into deeper fractures. In contrast, high-porosity rocks provide multiple connected pathways that facilitate deeper fluid penetration and more efficient oil displacement, thereby lowering flow resistance [47, 48]. Overall, adsorption and fracture connectivity jointly govern the flow resistance of displacing fluids in fractured reservoirs, while the inverse relationship between porosity and resistance indicates that enhanced connectivity is the dominant factor in reducing flow resistance [49].

The pore radius exerts a pronounced influence on the flow resistance of displacing fluids in reservoir fractures, as illustrated in Figure 10. The results indicate that flow resistance decreases with increasing pore radius, reflecting improved fluid mobility in larger pores. Specifically, when the pore radius is below 20 μm, flow resistance remains relatively high. Increasing the pore radius from 20 μm to 30 μm reduces the resistance from 33×10^{-3} N to 32×10^{-3} N, while a further increase to 40 μm results in a sharp decline of 8×10^{-3} N. This marked decrease is mainly attributed to the combined effects of adsorption and the Jamin effect.

At small pore radii, the enhanced contact between the displacing agent and the fracture surface promotes greater adsorption through the interaction of functional groups with the rock surface, thereby increasing flow resistance. In contrast, at larger pore radii, the reduced surface interaction limits material adsorption, leading to lower resistance. Meanwhile, the Jamin effect further intensifies flow resistance at small pore radii, as gel aggregates within the displacing fluid are prone to pore blockage, impeding flow [50]. When the pore radius is large, these aggregates can pass through more easily, minimizing blockage and resistance. Consequently, the synergistic effects of adsorption and the Jamin effect jointly account for the high flow resistance observed at small pore radii, which is unfavorable for oil recovery in low-permeability unconventional reservoirs [51, 52].

In summary, the adsorption of displacement agents

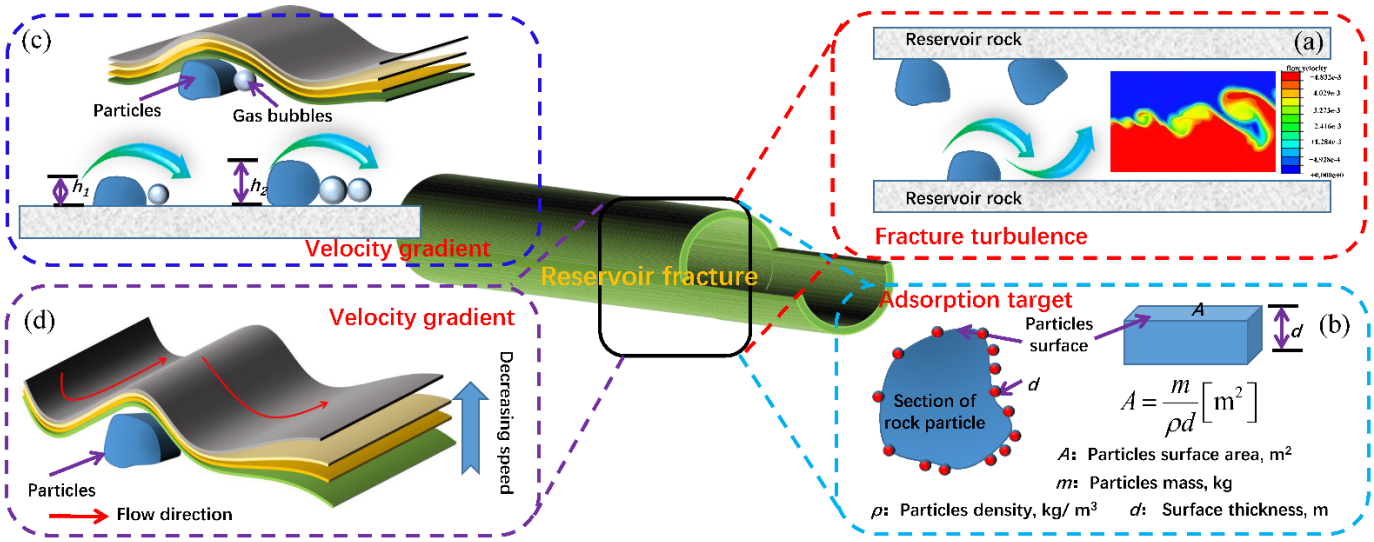

Figure 8. Mechanism of flow resistance revealed by particles on crack surface.

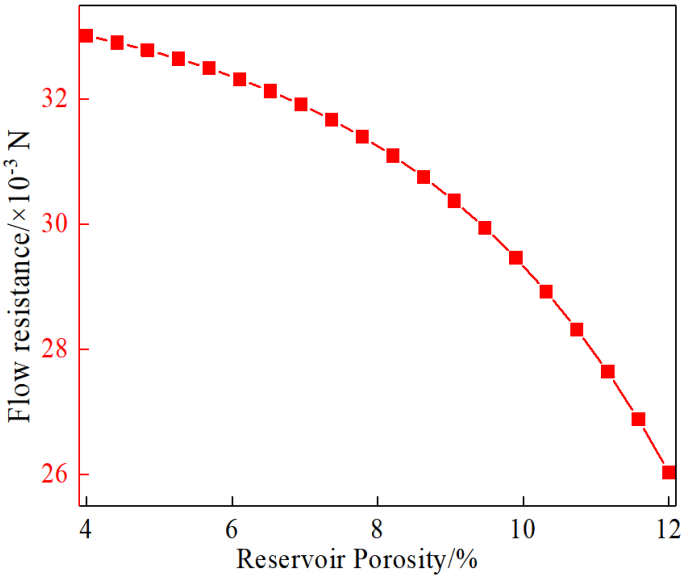

Figure 9. Changes in flow resistance of different reservoir porosities.

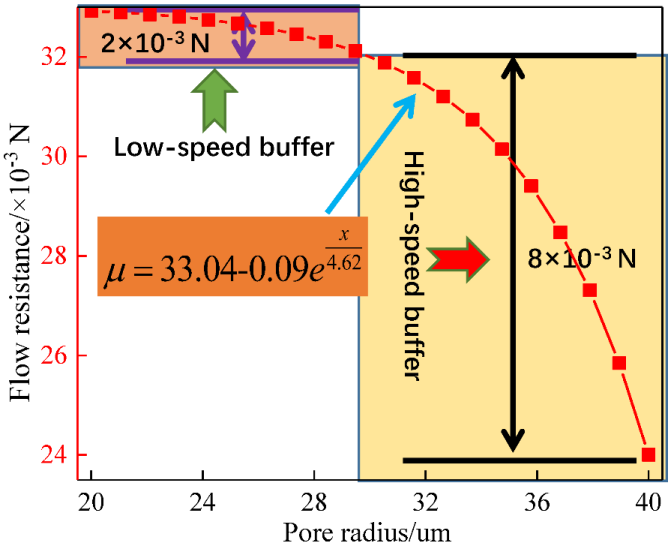

Figure 10. Changes in flow resistance of different reservoir pore radius.

on rock surfaces represents a critical factor governing flow resistance, offering important insights into the mechanisms of reservoir damage and recovery. In unconventional reservoirs, employing displacement agents with low adsorption affinity toward reservoir rocks can effectively enhance recovery efficiency. Nevertheless, reservoir damage remains a major contributor to flow resistance and requires further investigation.

3.3 Analysis of the Relationship Between Reservoir Damage and Flow Resistance

As previously discussed, adsorption plays a pivotal role in regulating the flow resistance of reservoir fluids and significantly contributes to reservoir damage. Accordingly, this study investigates the relationship between reservoir damage and flow resistance, employing adsorption effects to elucidate the mechanisms underlying their coupled variation. As shown in Figure 11, a distinct positive correlation exists between flow resistance and reservoir damage, indicating that higher flow resistance is accompanied by more severe formation damage and a pronounced reduction in permeability (as expressed in Equation 10). Figure 11 further demonstrates an inverse correlation between permeability and flow resistance. When the flow resistance is 33 × 10^{-3} N, the corresponding reservoir damage rate and permeability are 9% and 3 mD, respectively. Increasing the flow

resistance to 35 × 10^{-3} N raises the damage rate to 10% and decreases the permeability to 2.6 mD.

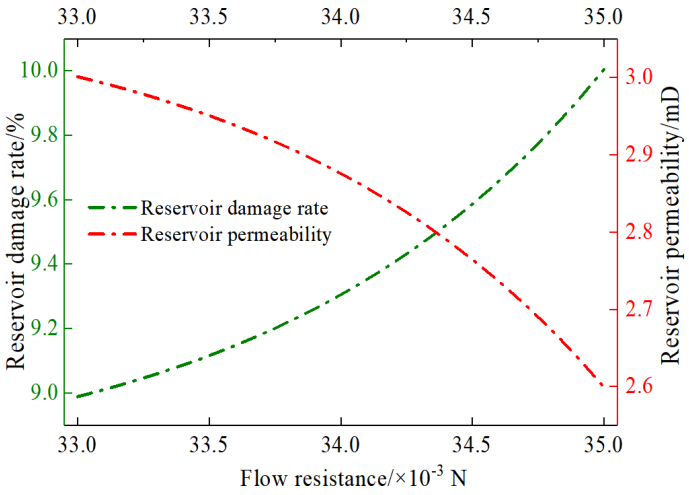

Figure 11. Relationship curve between reservoir damage rate, reservoir permeability and flow resistance.

The interdependence among these three parameters—flow resistance, reservoir damage, and permeability—originates from the adsorption of chemical agents in the displacing fluid onto the rock surface and the subsequent pore-sealing effect of colloidal substances. Lower flow resistance corresponds to weaker adsorption and reduced blockage within reservoir fractures, whereas stronger adsorption at higher flow resistance leads to a significant decline in permeability due to fracture surface occlusion. Additionally, the entrapment of colloidal materials within pore throats, driven by the Jamin effect, further amplifies this relationship. Therefore, the flow resistance of displacing fluids within reservoir fractures is intrinsically linked to reservoir damage, providing crucial guidance for optimizing fluid migration, enhancing oil recovery efficiency, and mitigating formation impairment in geological reservoirs [53].

$$g = \frac{K_1 - K_2}{K_1} \times 100\% \tag{10}$$

where g is the reservoir damage rate, %. K_1 and K_2 are the initial permeability of reservoir core and permeability after oil displacement.

At the same time, it is observed that the flow resistance in Figure 11 ceases to increase, which may be attributed to variations in reservoir permeability. Such variations are closely associated with the adsorption type of the oil-displacing agent on the rock surface, as this adsorption behavior directly governs changes in the internal pore volume and effective flow radius of reservoir fractures [54, 55]. The corresponding trends in flow resistance and permeability in Figure 11 clearly indicate that the adsorption of the oil-displacing agent on the rock surface follows a monolayer Langmuir adsorption pattern. This phenomenon arises because once the active adsorption sites on the rock surface are occupied by the functional groups of the oil-displacing agent, additional adsorption becomes thermodynamically unfavorable [56, 57]. Consequently, the remaining oil-displacing agents near the rock surface, lacking available adsorption sites, are carried away with the flowing displacement fluid, thereby preventing further increases in flow resistance.

3.4 Flow Resistance and Oil Displacement Efficiency

Figure 12 summarizes the effect of flow resistance on oil recovery efficiency in geological reservoirs. Low flow resistance clearly enhances recovery efficiency. As shown in Figure 12, assuming a uniform fracture network and a homogeneous reservoir, weak flow resistance results in only a slight increase in oil recovery efficiency. When flow resistance rises from 33 × 10^{-3} N to 36 × 10^{-3} N, the recovery efficiency decreases by merely 4%. However, at higher resistance, the efficiency drops rapidly, likely because increased reservoir resistance reduces the flow velocity of the recovery fluid within fractures, hindering crude oil displacement.

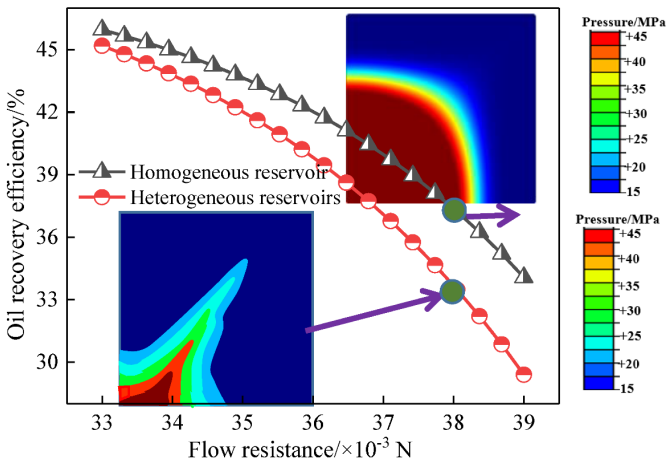

Figure 12. Relationship curve between flow resistance of displacement fluid and displacement efficiency.

In heterogeneous, single-fracture reservoirs, oil recovery efficiency declines more sharply under the same flow resistance, which may be attributed to the fingering behavior of the recovery fluid. The fluid preferentially migrates through zones of higher

permeability and porosity, exacerbating channeling effects. In contrast, homogeneous reservoirs promote more uniform displacement under identical resistance, improving overall recovery. Therefore, although flow resistance and recovery efficiency exhibit an inverse relationship, reservoir heterogeneity remains a key factor influencing recovery performance.

4 Conclusion

The comprehensive performance evaluation device developed in this study enables systematic assessment of the physicochemical and flow properties of oil-displacing fluids under reservoir conditions. This provides robust data support for selecting appropriate displacement fluids tailored to specific reservoir parameters, thereby enhancing oil recovery efficiency. The newly synthesized oil-displacing agent demonstrates lower flow resistance and higher viscosity than commercial counterparts, both of which are critical for improving recovery performance in geological reservoirs. Moreover, this study incorporates adsorption mechanisms into the understanding of flow resistance regulation within reservoir fractures, offering new strategies for optimizing displacement fluid flow behavior. Overall, the findings establish a foundational dataset for evaluating oil-displacing fluid behavior across reservoirs with varying geological conditions, facilitating the formulation of effective field-scale recovery strategies. However, the practical application of the synthesized oil-displacing agent in actual reservoir environments has not yet been verified, which represents a key direction for future research.

Data Availability Statement

Data will be made available on request.

Funding

This work was supported without any funding.

Conflicts of Interest

Wusheng Li is affiliated with the Directional Well Drilling Company of Bohai Drilling Engineering Co., Ltd, CNPC, Tianjin 300385, China. The authors declare that this affiliation had no influence on the study design, data collection, analysis, interpretation, or the decision to publish, and that no other competing interests exist.

AI Use Statement

The authors declare that no generative AI was used in the preparation of this manuscript.

Ethical Approval and Consent to Participate

Not applicable.

References

[1] Wang, Y., Han, X., Li, J., Liu, R., Wang, Q., Huang, C., ... & Lin, R. (2023). Review on oil displacement technologies of enhanced oil recovery: state-of-the-art and outlook. *Energy & Fuels, 37*(4), 2539-2568. [CrossRef]

[2] Wei, B., Romero-Zerón, L., & Rodrigue, D. (2014). Oil displacement mechanisms of viscoelastic polymers in enhanced oil recovery (EOR): a review. *Journal of Petroleum Exploration and Production Technology, 4*(2), 113-121. [CrossRef]

[3] Basu, S., Nandakumar, K., & Masliyah, J. H. (1996). A study of oil displacement on model surfaces. *Journal of colloid and interface science, 182*(1), 82-94. [CrossRef]

[4] Cao, W., Xie, K., Lu, X., Liu, Y., & Zhang, Y. (2019). Effect of profile-control oil-displacement agent on increasing oil recovery and its mechanism. *Fuel, 237*, 1151-1160. [CrossRef]

[5] Shuhong, J., Changbing, T., Chengfang, S. H. I., Jigen, Y. E., & Xiujuan, F. U. (2012). New understanding on water-oil displacement efficiency in a high water-cut stage. *Petroleum Exploration and Development, 39*(3), 362-370. [CrossRef]

[6] Conn, C. A., Ma, K., Hirasaki, G. J., & Biswal, S. L. (2014). Visualizing oil displacement with foam in a microfluidic device with permeability contrast. *Lab on a Chip, 14*(20), 3968-3977. [CrossRef]

[7] Tan, F., Jiang, R., Ma, C., Jing, Y., Chen, K., & Lu, Y. (2025). CO2 oil displacement and geological storage status and prospects. *Energy Science & Engineering, 13*(2), 475–511. [CrossRef]

[8] Yikun, L. I. U., Fengjiao, W. A. N. G., Yumei, W. A. N. G., Binhui, L. I., Guang, Y. A. N. G., Jiqiang, Z. H. I., ... & He, X. U. (2022). The mechanism of hydraulic fracturing assisted oil displacement to enhance oil recovery in low and medium permeability reservoirs. *Petroleum Exploration and Development, 49*(4), 864-873. [CrossRef]

[9] Chen, L., Zhang, G., Ge, J., Jiang, P., Tang, J., & Liu, Y. (2013). Research of the heavy oil displacement mechanism by using alkaline/surfactant flooding system. *Colloids and Surfaces A: Physicochemical and Engineering Aspects, 434*, 63–71. [CrossRef]

[10] Hua, Z., Lin, M., Dong, Z., Li, M., Zhang, G., & Yang, J. (2014). Study of deep profile control and oil displacement technologies with nanoscale polymer microspheres. *Journal of colloid and interface science, 424*, 67-74. [CrossRef]

[11] Lai, N., Zhao, J., Zhu, Y., Wen, Y., Huang, Y., & Han, J. (2021). Influence of different oil types on the stability and oil displacement performance of gel foams. *Colloids and Surfaces A: Physicochemical and Engineering Aspects, 630*, 127674. [CrossRef]

[12] Comiti, F., Cadol, D., & Wohl, E. (2009). Flow regimes, bed morphology, and flow resistance in self-formed step-pool channels. *Water Resources Research, 45*(4), W04424. [CrossRef]

[13] Xu, Y., Sheng, G., Zhao, H., Hui, Y., Zhou, Y., Ma, J., Rao, X., Zhong, X., & Gong, J. (2021). A new approach for gas–water flow simulation in multi-fractured horizontal wells of shale gas reservoirs. *Journal of Petroleum Science and Engineering, 199*, 108292. [CrossRef]

[14] Cornelissen, P., & Jansen, J. D. (2023). Steady-state flow through a subsurface reservoir with a displaced fault and its poro-elastic effects on fault stresses. *Transport in Porous Media, 150*(3), 709–734. [CrossRef]

[15] Deng, X., Li, S., Guan, B., Li, J., Meng, X., Wei, H., & Wang, Z. (2025). Study on the influence of reservoir wettability on shale oil flow characteristics by molecular dynamics simulation. *Arabian Journal for Science and Engineering, 50*(7), 4643-4660. [CrossRef]

[16] Wang, Q., Zhou, F., Su, H., Zhang, S., Dong, R., Yang, D., ... & Li, J. (2024). Experimental evaluations of nano high-viscosity friction reducers to improve acid fracturing efficiency in low-permeability carbonate reservoirs. *Chemical Engineering Journal, 483*, 149358. [CrossRef]

[17] Palmer, T. L., Espås, T. A., & Skartlien, R. (2019). Effects of polymer adsorption on the effective viscosity in microchannel flows: phenomenological slip layer model from molecular simulations. *Journal of Dispersion Science and Technology, 40*(2), 264-275. [CrossRef]

[18] Song, H., Lao, J., Zhang, L., Xie, C., & Wang, Y. (2023). Underground hydrogen storage in reservoirs: pore-scale mechanisms and optimization of storage capacity and efficiency. *Applied energy, 337*, 120901. [CrossRef]

[19] Zhu, W., Liu, Y., Li, Z., Yue, M., & Kong, D. (2021). Study on pressure propagation in tight oil reservoirs with stimulated reservoir volume development. *ACS omega, 6*(4), 2589-2600. [CrossRef]

[20] Lei, M., Huang, W. A., Li, N., Jia, J. H., Li, J. X., Wang, Y. W., & Li, J. Y. (2017). The damage mechanism of oil-based drilling fluid for tight sandstone gas reservoir and its optimization. *Journal of Petroleum Science and Engineering, 158*, 616-625. [CrossRef]

[21] Chen, F., Wang, Z., Fu, S., Li, A., & Zhong, J. (2023). Research on transformation of connate water to movable water in water-bearing tight gas reservoirs. *Energies, 16*(19), 6961. [CrossRef]

[22] Yang, S., Sheng, Q., Zou, M., & Zheng, Q. (2025). Fractal study on spontaneous imbibition characteristics of the non-Newtonian fracturing fluids in porous media with rough surfaces. *Chinese Journal of Physics, 95*, 1155-1166. [CrossRef]

[23] Dang, C., Liu, S., Chen, Q., Sun, W., Zhong, H., Hu, J., ... & Ni, J. (2021). Response of microbial nitrogen transformation processes to antibiotic stress in a drinking water reservoir. *Science of The Total Environment, 797*, 149119. [CrossRef]

[24] Yoon, W. W., Han, W. S., Hwang, J., Kim, J. W., Chang, K. W., & Suk, H. (2024). Effect of fracture characteristics on groundwater flow adjacent to high-level radioactive waste repository. *Journal of Hydrology, 629*, 130593. [CrossRef]

[25] Xu, J., Qin, H., & Li, H. (2022). The Laplace-transform embedded discrete fracture model for flow simulation of stimulated reservoir volume. *Journal of Petroleum Exploration and Production Technology, 12*(8), 2303-2328. [CrossRef]

[26] Deng, J., Zhu, W., & Ma, Q. (2014). A new seepage model for shale gas reservoir and productivity analysis of fractured well. *Fuel, 124*, 232-240. [CrossRef]

[27] Wu, Z., Cui, C., Jia, P., Wang, Z., & Sui, Y. (2022). Advances and challenges in hydraulic fracturing of tight reservoirs: A critical review. *Energy Geoscience, 3*(4), 427-435. [CrossRef]

[28] Zhao, L., Chen, X., Zou, H., Liu, P., Liang, C., Zhang, N., ... & Du, J. (2020). A review of diverting agents for reservoir stimulation. *Journal of Petroleum Science and Engineering, 187*, 106734. [CrossRef]

[29] Kostic, S., & Parker, G. (2003). Progradational sand-mud deltas in lakes and reservoirs. Part 1. Theory and numerical modeling. *Journal of Hydraulic Research, 41*(2), 127-140. [CrossRef]

[30] Wang, T., Zhang, Y., Li, L., Yang, Z., Liu, Y., Fang, J., ... & You, Q. (2018). Experimental study on pressure-decreasing performance and mechanism of nanoparticles in low permeability reservoir. *Journal of Petroleum Science and Engineering, 166*, 693-703. [CrossRef]

[31] Xie, Y., Liao, J., Zhao, P., Xia, K., & Li, C. (2024). Effects of fracture evolution and non-Darcy flow on the thermal performance of enhanced geothermal system in 3D complex fractured rock. *International Journal of Mining Science and Technology, 34*(4), 443-459. [CrossRef]

[32] Hu, A., Su, L., Cao, G., Luo, Z., Yan, C., & Chen, Q. (2025). Experimental Study on the Effect of Fractures on the Irreducible and Movable Water in Water-Bearing Tight Sandstone Gas Reservoirs. *Processes, 13*(6), 1685. [CrossRef]

[33] Zhang, Q., Liu, H., Kang, X., Liu, Y., Dong, X., Wang, Y., Liu, S., & Li, G. (2021). An investigation of production performance by cyclic steam stimulation using horizontal well in heavy oil reservoirs. *Energy, 218*, 119500. [CrossRef]

[34] Li, B., Su, Y., & Wang, W. (2017). Temporal scale-based

production analysis of fractured horizontal wells with stimulated reservoir volume. *Journal of Natural Gas Science and Engineering, 48*, 46–64. [CrossRef]

[35] Cao, H., Xia, Y., Wang, J., Ji, H., Hong, H., Xu, K., ... & Xu, Z. (2025). Shearing metal-organic framework lattice defects create low-resistance reservoir channels for high-performance aqueous organic flow battery. *Journal of Membrane Science, 717*, 123607. [CrossRef]

[36] Zhao, Y. L., Zhang, L. H., Liu, Y. H., Hu, S. Y., & Liu, Q. G. (2015). Transient pressure analysis of fractured well in bi-zonal gas reservoirs. *Journal of Hydrology, 524*, 89–99. [CrossRef]

[37] Wang, P., Hu, Y. H., Zhang, L. Y., Meng, Y., Ma, Z. F., Wang, T. R., ... & Zhang, Y. (2024). Experimental study of the influencing factors and mechanisms of the pressure-reduction and augmented injection effect by nanoparticles in ultra-low permeability reservoirs. *Petroleum Science, 21*(3), 1915-1927. [CrossRef]

[38] Jia, P., Wu, D., Yin, H., Li, Z., Cheng, L., & Ke, X. (2021). A practical solution model for transient pressure behavior of multistage fractured horizontal wells with finite conductivity in tight oil reservoirs. *Geofluids, 2021*(1), 9948505. [CrossRef]

[39] Xin, Y., Li, B., Li, Z., Li, Z., Wang, B., Wang, X., ... & Li, W. (2025). Gas channeling control with CO2-responsive gel system in fractured low-permeability reservoirs: Enhancing oil recovery during CO2 flooding. *Separation and Purification Technology, 353*, 128475. [CrossRef]

[40] Cui, Q., Zhao, Y., Bu, C., Zheng, J., Hu, H., & Zhang, L. (2023). A hybrid numerical/analytical model of transient seepage for vertical fractured well in tight gas reservoir by use of fractal theory and conformal mapping method. *Fractals, 31*(08), 2340180. [CrossRef]

[41] Guo, J., Cao, W., Wang, Y., & Jiang, F. (2019). A novel flow-resistor network model for characterizing enhanced geothermal system heat reservoir. *Frontiers in energy, 13*(1), 99-106. [CrossRef]

[42] Huang, T., Liu, T., Zhai, C., Sun, Y., Xu, J., Li, Y., & Xu, H. (2025). Nonlinear flow and permeability characteristics in fracture induced by shale self-supporting particles. *Energy & Fuels, 39*(10), 4746-4760. [CrossRef]

[43] Lv, J. X., & Hou, B. (2024). Fractures interaction and propagation mechanism of multi-cluster fracturing on laminated shale oil reservoir. *Petroleum Science, 21*(4), 2600-2613. [CrossRef]

[44] Dai, Z., Zhang, A., Wang, S., Fu, X., Yang, L., Jiang, X., & Wang, H. (2023). The development characteristics and mechanisms of the Xigou debris flow in the Three Gorges Reservoir Region. *Frontiers in Earth Science, 11*, 1122562. [CrossRef]

[45] Zhang, X., Li, L., Da, Q. A., Su, Y., Ma, S., & Zhu, Z. (2022). Microfluidic investigation on multiphase interaction and flow behavior of immiscible/miscible gases in deep heterogeneous reservoir. *Journal of Environmental Chemical Engineering, 10*(6), 109036. [CrossRef]

[46] Chen, D., Yang, F., Li, H., Wei, C., Yang, M., Zhao, X., ... & Li, J. (2024). Study on Water Intrusion Flow Model of the Tight Gas Reservoir. *Chemistry and Technology of Fuels and Oils, 60*(2), 297-308. [CrossRef]

[47] Xu, Z., Zhao, M., Zhang, Y., Wang, P., Wu, Y., Li, L., ... & Dai, C. (2023). Bio-inspired superhydrophobic interface of nano-gaseous film for reducing injection pressure in oil reservoirs. *Chemical Engineering Journal, 454*, 140393. [CrossRef]

[48] Su, Y., Li, M., Wang, W., & Dong, M. (2021). Fractal-based production analysis for shale reservoir considering vertical cross-flow. *Fractals, 29*(08), 2150251. [CrossRef]

[49] Zhang, L., Khan, N., & Pu, C. (2019). A new method of plugging the fracture to enhance oil production for fractured oil reservoir using gel particles and the HPAM/Cr3+ system. *Polymers, 11*(3), 446. [CrossRef]

[50] Liu, Q., Chen, Y., Wang, W., Liu, H., Hu, X., & Xie, Y. (2017). A productivity prediction model for multiple fractured horizontal wells in shale gas reservoirs. *Journal of Natural Gas Science and Engineering, 42*, 252-261. [CrossRef]

[51] Knauss, W. G. (2015). A review of fracture in viscoelastic materials. *International Journal of Fracture, 196*(1), 99-146. [CrossRef]

[52] Zhang, L., Gao, J., Hu, S., Guo, J., & Liu, Q. (2016). Five-region flow model for MFHWs in dual porous shale gas reservoirs. *Journal of Natural Gas Science and Engineering, 33*, 1316-1323. [CrossRef]

[53] Weiyao, Z. H. U., Qian, Q. I., Qian, M. A., Jia, D. E. N. G., Ming, Y. U. E., & Yuzhang, L. I. U. (2016). Unstable seepage modeling and pressure propagation of shale gas reservoirs. *Petroleum Exploration and Development, 43*(2), 285-292. [CrossRef]

[54] Wei, Y., Jia, A., He, D., & Wang, J. (2016). A new method in predicting productivity of multi-stage fractured horizontal well in tight gas reservoirs. *Journal of Natural Gas Geoscience, 1*(5), 397-406. [CrossRef]

[55] Belikov, V. V., & Borisova, N. M. (2023). Numerical 2D-Modeling of Rain Runoff Transformation in the Drainage Basin of Gelendzhik City Taking into Account the Mountain Collector and Accumulating Reservoirs. *Water Resources, 50*(4), 482-490. [CrossRef]

[56] Liu, X., Liu, W., Chen, X., Wang, L., Zhang, Z., & Peng, T. (2024). Estimating fracture characteristics and hydraulic conductivity from slug tests in epikarst of southwest China. *Journal of Hydrology: Regional Studies, 53*, 101777. [CrossRef]

[57] Gao, X., Guo, K., Chen, P., Yang, H., & Zhu, G. (2023). A productivity prediction method for multi-fractured horizontal wells in tight oil reservoirs considering fracture closure. *Journal of Petroleum Exploration and Production Technology, 13*(3), 865-876. [CrossRef]

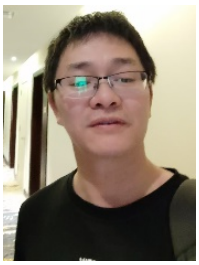

Wusheng Li graduated from Northeast Petroleum University with a bachelor's degree and currently works at China National Petroleum Corporation Bohai Drilling Directional Well Technical Service Branch, where he is mainly engaged in underground drilling and fault analysis during the drilling process. (Email: 313010984@qq.com)

Junying Liao earned her undergraduate degree in Mechanical Design, Manufacturing and Automation from the China University of Petroleum (Beijing) Karamay Campus, and in 2024 she began her master's program in Mechanical Engineering at the same university. (Email: 2024216931@st.cupk.edu.cn)